Journal of Bioscience and Bioengineering
VOL. 128 No. 1, 13–21, 2019

ELSEVIER

www.elsevier.com/locate/jbiosc

# Expression of alcohol oxidase gene from *Ochrobactrum* sp. AIU 033 in recombinant *Escherichia coli* through the twin-arginine translocation pathway

Kenji Matsumura, Miwa Yamada,* Takeshi Yamashita, Hitomi Muto, Ken-ichi Nishiyama, Hitoshi Shimoi, and Kimiyasu Isobe

*Department of Biological Chemistry and Food Science, Iwate University, Ueda-3, Morioka 020-8550, Japan*

Received 29 October 2018; accepted 20 December 2018
Available online 28 January 2019

**We cloned a set of genes encoding alcohol oxidase from *Ochrobactrum* sp. AIU 033 (OcAOD), which exhibits the appropriate substrate specificity for glyoxylic acid production from glycolic acid. The set of genes for OcAOD contained two open reading frames consisting of 555-bp (*aodB*) and 1572-bp (*aodA*) nucleotides, which encode the precursor for the β-subunit and α-subunit of OcAOD, respectively. We expressed the cloned genes as an active product in *Escherichia coli* BL21(DE3). The recombinant OcAOD oxidized glycolic acid and primary alcohols with C2–C8 but not glyoxylic acid (as is the case for native OcAOD), whereas the $K_m$ and $V_{max}$ values for glycolic acid and the pH stability were higher than those of native OcAOD. A consensus sequence for the twin-arginine translocation (Tat) pathway was identified in the N-terminal region of the precursor for the β-subunit, and the active form of OcAOD was localized in the periplasm of recombinant *E. coli*, which indicated that OcAOD would be transported from the cytoplasm to the periplasm by the hitchhiker mechanism through the Tat pathway. The OcAOD productivity of the recombinant *E. coli* was 24-fold higher than that of *Ochrobactrum* sp. AIU 033, and it was further enhanced by 1.2 times by the co-expression of additional *tatABC* from *E. coli* BL21(DE3). Our findings thus suggest a function of the β-subunit of OcAOD in membrane translocation, and that the recombinant OcAOD has characteristics that are suitable for the enzymatic synthesis of glyoxylic acid as well as native OcAOD.**



[**Key words:** Alcohol oxidase; Ethylene glycol; Glycolic acid; Glyoxylic acid; Twin-arginine translocation pathway]

Glyoxylic acid is a beneficial raw material for the chemical synthesis of vanillin, which is used as a flavor and fragrance ingredient as well as in the manufacture of pharmaceuticals and agrochemicals (1). Glyoxylic acid is commonly manufactured by nitric acid oxidation from glyoxal, and this chemical synthesis requires a large amount of neutralizer and produces by-products such as oxalate. Thus, biochemical methods have been developed to produce glyoxylic acid from glycolic acid with the use of glycolic acid oxidases, because these enzyme reactions do not utilize nitric acid (2–4). In these biochemical processes for glyoxylic acid production, glycolic acid is used as a starting material and the glycolic acid oxidases are prepared from plants. However, glycolic acid is more expensive than glyoxal, and it is difficult to obtain enzymes from plants throughout an entire year. It is worth noting that a combination of ethylene glycol and microbial oxidases is used in a method for the enzymatic production of glyoxylic acid, because microbial enzymes are easily obtained and an ethylene glycol is inexpensive material compared to glycolic acid (5,6).

Our group has proposed two pathways for the production of glyoxylic acid from ethylene glycol via glycolic acid or glyoxal (Fig. 1) (7). To date, our group has found the following microbial enzymes suitable for each of the two routes. The enzymes that oxidize ethylene glycol into glyoxal via glycolaldehyde were identified in alcohol oxidase (AOD, EC 1.1.3.13) from methylotrophic yeast (8) and glycerol oxidase was identified from *Aspergillus japonicus* (5) (Fig. 1, reactions 1 and 4). The enzymes that oxidize ethylene glycol were also isolated from AODs from *Aspergillus ochraceus* AIU 031 (9) and *Penicillium purpurescens* AIU 063 (10) (Fig. 1, reaction 1).

The enzyme that oxidized glycolaldehyde into glyoxal was found from *Paenibacillus* sp. AIU 311 (11) and *P. purpurescens* AIU 063 (10) (Fig. 1, reaction 4). The oxidases that catalyze the oxidation of glyoxal into glyoxylic acid were isolated from *Pseudomonas* sp. AIU 362 (12) (Fig. 1, reaction 5). The aldehyde oxidase that catalyzes the conversion of glycolaldehyde to glycolic acid was isolated from *Burkholderia* sp. AIU 129 (13) (Fig. 1, reaction 2). Glycolate dehydrogenase from *Trichoderma harzianum* AIU 353 (14) and glycerol oxidase from *A. japonicus* (5) were reported to catalyze the conversion of glycolic acid into glyoxylic acid (Fig. 1, reaction 3).

We further isolated a novel type of AOD from *Ochrobactrum* sp. AIU 033 (OcAOD) which belongs to gram-negative bacteria (7) (Fig. 1, reaction 3). The OcAOD showed oxidase activity for glycolic acid and primary alcohols of C2–C10, but not for glyoxylic acid. This substrate specificity is remarkably advantageous for glyoxylic acid production, because the reaction product, glyoxylic acid, was not further oxidized to oxalic acid. We have therefore studied the characteristics of OcAOD in detail. The enzyme has an $\alpha_2\beta_2$ hetero subunit structure in which the α-subunit is 52 kDa and

* Corresponding author. Tel./fax: +81 19 621 6159.
*E-mail address:* myamada@iwate-u.ac.jp (M. Yamada).

1389-1723/$ – see front matter 
https://doi.org/10.1016/j.jbiosc.2018.12.012

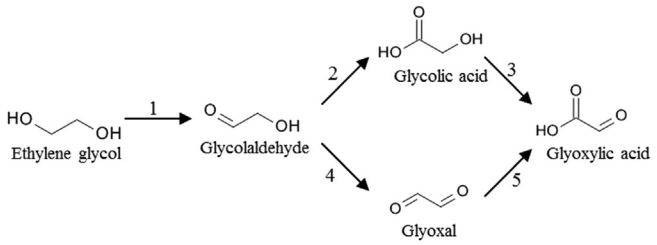


FIG. 1. Proposed pathways of glyoxylic acid production from ethylene glycol.

the β-subunit is 14 kDa, and it contains flavin and iron atom as cofactors (7). The function of each subunit has not been elucidated yet.

To clarify the function of subunits of OcAOD, we conducted the present study to perform the gene cloning, sequencing, and expression of the set of genes for OcAOD in recombinant *Escherichia coli*, and we characterized the recombinant OcAOD enzyme. Since a signal motif for the twin-arginine translocation (Tat) pathway was detected in the N-terminal region of the precursor for the β-subunit, we also investigated the localization of OcAOD in an expression host, *E. coli* and the effect of the co-expression of *tatABC* and the set of genes for OcAOD on the enzyme's productivity.

## MATERIALS AND METHODS

**Chemicals** Sodium glycolate was purchased from Wako Pure Chemical Industries (Osaka, Japan). Horseradish peroxidase (EC 1.11.1.7) was obtained from Amano Enzyme (Nagoya, Japan). All other chemicals used were the highest grade that is commercially available. The enzymes for genetic engineering were purchased from Takara Bio (Shiga, Japan) or Toyobo (Osaka, Japan) and used as recommended by the supplier.

**Medium and culture conditions** *Ochrobactrum* sp. AIU 033, which is a source of genomic DNA, was incubated with a 1,2-propanediol medium consisting of 1% 1,2-propanediol, 0.2% $(NH_4)_2SO_4$, 0.1% $K_2HPO_4$, 0.1% $NaH_2PO_4 \cdot 2H_2O$, 0.05% $MgSO_4 \cdot 7H_2O$, 0.02% $CaCl_2 \cdot 2H_2O$, 0.5% corn steep liquor, and 0.05% yeast extract (pH 6.0) at 30°C for 2 days with shaking (120 strokes/min) (7).

*E. coli* JM109, which was used for plasmid construction, was cultured in a Luria–Bertani (LB) medium (1% peptone, 0.5% yeast extract, and 1% NaCl, pH 7.0) containing ampicillin (100 μg/mL) at 30°C.

**Gene cloning and construction of the plasmid for the expression of the set of genes for OcAOD** Standard recombinant DNA manipulation was used for the isolation of plasmid DNA (15). As mentioned in our report (7), OcAOD has a molecular mass of 130 kDa and has an $\alpha_2\beta_2$ structure in which the α-subunit is 52 kDa and the β-subunit is 14 kDa. The N-terminal amino acid sequences (30 residues) of the α- and β-subunits showed high similarity to those of the putative glucose-methanol-choline (GMC) oxidoreductase of *Ochrobactrum anthropi* ATCC 49188 (97% identity) and the hypothetical protein of *O. anthropi* ATCC 49188 (97% identity), respectively (7).

In the genomic DNA of *O. anthropi* ATCC 49188, the putative GMC oxidoreductase gene and hypothetical protein gene exist next to each other, and they are oriented in the same direction (16). We thus designed the following primers for polymerase chain reaction (PCR): Sense primer (S1) 5′-ATGACTACCGTTTTTGACGGT-3′ (the 5′-terminal sequence of the GMC oxidoreductase gene of *O. anthropi* ATCC 49188) and antisense primer (A1) 5′-TCAGATCGCCCCGCTTCTTC-3′ (the 3′-terminal sequence of the gene encoding the hypothetical protein of *O. anthropi* ATCC 49188) by referring to the genomic DNA sequence of *O. anthropi* ATCC 49188. The PCR was performed in 50 μl of LA PCR Buffer II ($Mg^{2+}$ free) containing 2.5 units of TaKaRa LA Taq DNA polymerase, 2.5 mM dNTP mixture, 2.5 mM $MgCl_2$, 0.5 μM each primer, and 0.5 μg of the genomic DNA extracted from *Ochrobactrum* sp. AIU 033 with the use of a Bacteria genomicPrep Mini Spin Kit (GE Healthcare UK, Buckinghamshire, UK). The reaction was followed by 30 cycles of amplification (a denaturation step at 98°C for 10 s, an annealing step at 55°C for 30 s, and an extension step at 72°C for 3 min). The 2293-bp DNA fragment was amplified and ligated to a pTA plasmid (Toyobo) containing a T7 promoter sequence by TA cloning. We named the resultant plasmid pTA-OcAOD (Fig. S1A).

To analyze the deletion effects of ORF1(*aodB*), we prepared pTA-OcAOD(Δ*aodB*) by PCR using the forward primer 5′-GGGAGGAAACAATGGCTGC-3′ and the reverse primer 5′-GTATTGGGAATTCGATATCAAG-3. pTA-OcAOD containing *aodB* and ORF2 (*aodA*) was used as a template for the PCR, which was carried out using a program of 30 cycles of 94°C for 2 min, 55°C for 30 s, and 72°C for 3 min. The PCR products were purified, phosphorylated by polynucleotide kinase, and self-ligated.

**Expression of the set of genes for OcAOD in recombinant *E. coli*** The recombinant *E. coli* BL21(DE3) harboring pTA-OcAOD or pTA-OcAOD(Δ*aodB*) was incubated in LB medium containing ampicillin (100 μg/mL) for 5 h, and then 0.1 mM isopropyl-β-D-thiogalactopyranoside (IPTG) was added to the culture medium. The cultivation was further continued for 20 h with shaking (120 strokes/min). The co-expression of the set of genes for OcAOD and *tatABC* was also performed under the same conditions.

**Purification of recombinant OcAOD** All of the purification procedures were performed at 5–10°C using potassium phosphate buffer, pH 6.0. First, 55.5 g of wet cells of *E. coli* BL21(DE3) harboring pTA-OcAOD from 10 L of culture broth was disrupted with glass beads in 10 mM buffer solution by a multi-beads shocker, and the supernatant (510 mL) collected by centrifugation at 10,000 ×*g* for 30 min was used as a crude enzyme solution. Then, solid ammonium sulfate (123 g) was added to the crude enzyme solution to reach 40% saturation with stirring, and the resulting precipitates were discarded by centrifugation.

The enzyme solution was applied onto a Phenyl-Toyopearl 650M column (20 cm × 3 cm diameter) (Tosoh, Tokyo, Japan) equilibrated with 10 mM buffer solution containing 3 M ammonium sulfate. The adsorbed enzyme was eluted by a linear gradient of 10 mM buffer solution containing 3 M ammonium sulfate and 0.5 M ammonium sulfate (500 mL each). The active fractions were collected and dialyzed against 10 mM buffer solution. The dialyzed enzyme solution was applied onto a GigaCap Q-Toyopearl 650 M column (11 cm × 3 cm diameter) (Tosoh) equilibrated with 30 mM buffer solution containing 50 mM NaCl.

The adsorbed enzyme was then eluted by a linear gradient of 30 mM buffer solution containing 50 mM NaCl and 180 mM NaCl (250 mL each). The active fractions were collected and dialyzed against 10 mM buffer solution and then applied to a Bio-Gel HTP hydroxyapatite column (11 cm × 1.8 cm diameter) (Bio-Rad Laboratories, Hercules, CA, USA) equilibrated with 0.2 M buffer solution. The adsorbed enzyme was eluted by a linear gradient of 0.2 M and 0.4 M buffer solution (125 mL each).

**Isolation of the spheroplast and periplasm fractions** All procedures were performed at 5°–10°C as described (17). The cells of *E. coli* BL21(DE3) harboring pTA-OcAOD in 100 mL of LB medium (0.8 absorbance at 600 nm) were harvested by centrifugation at 10,000 ×*g* for 5 min. The precipitate was rapidly resuspended in cold 0.75 M sucrose-10 mM Tris–HCl buffer, pH 7.8. Next, lysozyme was added to 100 μg/mL, and the mixture was allowed to stand in ice for 2 min. The suspension was slowly diluted with 2 volumes of cold 1.5 mM EDTA, pH 7.5. The supernatant solution (collected by centrifugation at 10,000 ×*g* for 5 min) was used for the enzyme activity measurement of the periplasm fraction after dialysis against 10 mM potassium phosphate buffer, pH 6.0. The precipitate was suspended in 1 mL of 10 mM potassium phosphate buffer (pH 6.0) again and disrupted with glass beads by a multi-beads shocker. The supernatant collected from this suspension by centrifugation at 10,000 ×*g* for 10 min was used for the enzyme activity measurement of the spheroplast fraction.

**Construction of the plasmid for the co-expression of the set of genes for OcAOD and *tatABC*** The pTA-OcAOD fragment was prepared by PCR in 50 μl of PCR Buffer for KOD-Plus (Toyobo) containing 1 unit of KOD-Plus polymerase, 0.2 mM of dNTP mixture, 1 mM of $MgSO_4$, 0.3 μM of each primer (i.e., the S2 and A2 primers), and 1 ng of the pTA-OcAOD plasmid. The amplification reaction was performed 30 cycles in the following conditions: a denaturation step at 94°C for 15 s, an annealing step at 56°C for 30 s, and an extension step at 68°C for 5 min 30 s.

The sequences of sense (S2) and antisense (A2) primers were 5′-TCACTGCCCGCTTCCAGT-3′ and 5′-ATGACCATGATTACGCCAAGC-3′, respectively. *tatABC* fragment was also obtained by PCR in 50 μl of PCR Buffer for KOD-Plus, containing 1 unit of KOD-Plus polymerase, 0.2 mM dNTP mixture, 1 mM $MgSO_4$, 0.3 μM each primer (i.e., the S3 and A3 primers), and 0.2 μg of the extracted genomic DNA from *E. coli* BL21(DE3). The sequences of the sense (S3) and antisense (A3) primers were 5′-CGTAATCATGGTCATAGGAAACAGCTATGGGTGGG-3′ and 5′-GAAGCGGGCAGTGCTCAGATAAAATATTTCTAGAT-3′, respectively.

The *tatABC* fragment was ligated to the pTA-OcAOD fragment amplified by PCR by an in-fusion reaction. We named the resultant plasmid pTA-OcAOD-TatABC (Fig. S1B), in which *tatABC* was located downstream of the set of genes for OcAOD.

**Assays of enzyme activity** We determined the oxidase activity for glycolic acid by measuring the rate of hydrogen peroxide formation at 30°C and pH 5.5, as we described (7). The dehydrogenase activity for 1,2-propanediol was assayed by following the NADH formation rate at 25°C and pH 9.5 (18). The β-lactamase activity was assayed by monitoring the absorbance at 482 nm, using nitrocefin as the substrate at 30°C and pH 7.0 (19).

**DNA sequencing analysis** To analyze the genes encoding OcAOD and confirm the new plasmid constructs, we performed DNA sequencing by the dideoxynucleotide chain-termination method with a Prism 310 Genetic Analyzer (Applied Biosystems, Foster City, CA, USA) using a BigDye terminator cycle sequencing ready reaction kit (Applied Biosystems). The nucleotide sequence was analyzed with GENETYX genetic information processing software (Software Development Co., Tokyo, Japan).


FIG. 2. The nucleotide sequence and the deduced amino acid (aa) sequence of the DNA fragment cloned from genomic DNA of *Ochrobactrum* sp. AIU 033. Underline, ORF1 (*aodB*); dotted underline, ORF2 (*aodA*); double underlining, putative signal peptides for the Tat pathway; boxes, predicted SD sequence, initiation codon, or stop codon; gray box, the consensus sequence for the Tat pathway; black box inside *aodB*, the aa sequence that is consistent with the N-terminal aa sequence of the β-subunit of native OcAOD (7); black box inside *aodA*, the aa sequence that is consistent with the N-terminal aa sequence of the α-subunit of native OcAOD (7). A1 indicates the position of the primer used for the cloning of the set of genes for OcAOD.

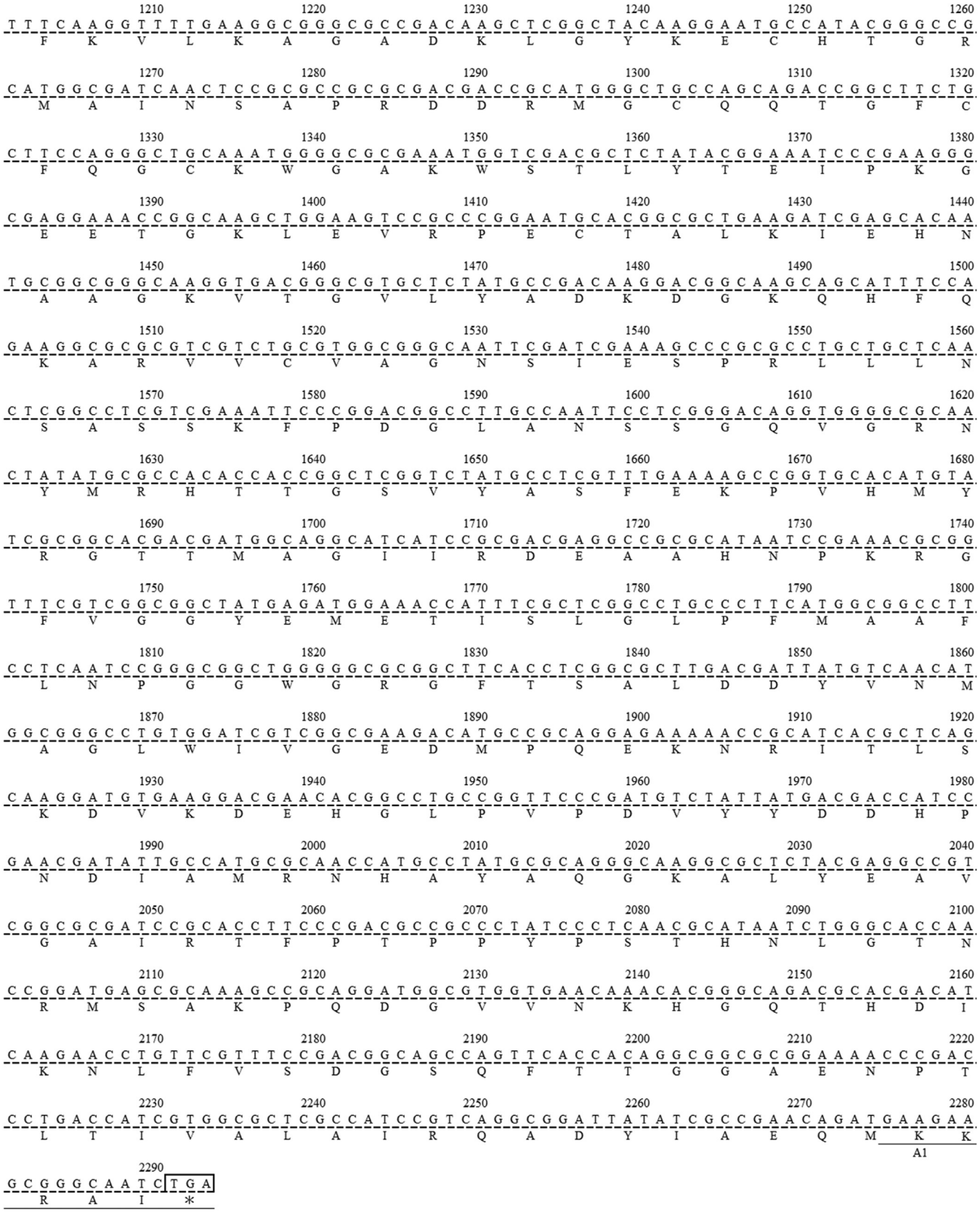


FIG. 2. (*continued*).

**Sodium dodecyl sulfate-polyacrylamide gel electrophoresis** The sample for sodium dodecyl sulfate-polyacrylamide gel electrophoresis (SDS-PAGE) was incubated with 1% SDS and 5% 2-mercaptoethanol at 100°C for 3 min. SDS-PAGE was performed according to the method of Laemmli (20). Proteins were stained with Coomassie Brilliant Blue R-250. The molecular mass of the denatured enzyme was estimated on the SDS-PAGE using the molecular marker standards of Bio-Rad Laboratories.

## RESULTS

**The cloning and sequencing of the set of genes for OcAOD** We obtained an approximately 2300-bp DNA fragment from genomic DNA of *Ochrobactrum* sp. AIU 033 by PCR using the S1 and A1 primers. These primers were designed based on the DNA sequence of *O. anthropi* ATCC 49188, the deduced proteins of which are homologous to those of OcAOD (see the Materials and methods section for details). Our sequence analysis of the amplified DNA fragment revealed a complementary sequence of A1 primer in the 3′-terminal region of the obtained DNA fragment (Fig. 2), but the sequence of the S1 primer was not confirmed in the 5′-terminal region of the DNA fragment. However, the amplified DNA fragment contained a 555-bp open reading frame (ORF1) at the position 71–625 of the amplified DNA fragment and a 1572-bp ORF (ORF2) at the position 722-2293 of the amplified DNA fragment, which encode a 184-amino acid (aa) polypeptide and a 523-aa polypeptide, respectively (Fig. 2). Both ORFs existed downstream of a predicted Shine–Dalgarno sequence.

Part of the deduced amino acid sequence in ORF 1 was completely identical to the N-terminal amino acid sequence of the β-subunit of native OcAOD, i.e., LETATLKPETMATLIQLAR-DIYPHDKLPDR (7) (Fig. 2, black box sequence inside the deduced amino acid sequence of ORF1). In addition, the deduced amino acid sequence of the N-terminal region of the ORF2 was identical to the N-terminal amino acid sequence of the α-subunit of the native OcAOD, i.e., AAPYDLKDDKVVVIIGSGAGGGTLGNELAQ (7) (Fig. 2, black box sequence inside the deduced amino acid sequence of ORF2). We therefore investigated the expressions of the set of these genes in recombinant *E. coli*.

**Expressions of cloning genes in recombinant *E. coli* BL21(DE3)** The recombinant *E. coli* BL21(DE3) strain harboring pTA-OcAOD, which contains ORF1 and OFR2, produced 222 munits of glycolic acid oxidase activity in the cells of 1 L of culture broth by IPTG induction. This productivity was 24 times higher than that of *Ochrobactrum* sp. AIU 033 (Table 1). However, when only ORF2 was expressed in recombinant *E. coli* using the pTA-OcAOD(Δ*aodB*) plasmid, glycolic acid oxidase activity was not detected (Table 1), indicating that both ORF1 and ORF2 are required for the production of active enzyme.

**Purification of the recombinant enzymes** We purified the recombinant enzymes derived from ORF1 and OFR2 to a homogeneous state with an overall yield of 0.3% by ammonium sulfate fractionation and three column chromatographies (Table S1). The molecular mass values of the recombinant enzymes were estimated as 52 kDa and 14 kDa on SDS-PAGE (Fig. 3), which is in agreement with those of the α- and β-subunits of native OcAOD, respectively. The specific activity was 8.0 munits/mg of protein in glycolic acid oxidase activity, which was twice that of native OcAOD (7). We then investigated some of the purified enzymes' characteristics.

**Substrate specificity of the recombinant enzyme** The recombinant enzyme oxidized glycolic acid and primary alcohols such as ethanol, 1-propanol, 1-butanol, 1-pentanol, 1-hexanol, and 1-octanol, but not glyoxylic acid or methanol (Table 2). Among these substrates, the oxidation rate of glycolic acid was faster than those of ethanol and 1-propanol, but slower than those of medium- and long-chain primary alcohols (C4–C8). This substrate specificity shows a trend that is similar to that of native OcAOD (7).

**TABLE 1.** Enzyme productivity of *Ochrobactrum* sp. AIU 033 and recombinant *E. coli* BL21(DE3) harboring the set of genes for OcAOD.

| Strain | Glycolic acid oxidase activity (mU/L broth)[c] |
|---|---|
| *E. coli* BL21(DE3)/pTA-OcAOD[a] | 222 ± 13.0 |
| *E. coli* BL21(DE3)/pTA-OcAOD(Δ*aodB*)[a] | 0 |
| *E. coli* BL21(DE3)/pTA-OcAOD-TatABC[a] | 265 ± 35.4 |
| *Ochrobactrum* sp. AIU 033[b] | 9.13 ± 1.07 |

[a] Recombinant *E. coli* BL21(DE3) harboring pTA-OcAOD, pTA-OcAOD(Δ*aodB*), or pTA-OcAOD-TatABC was incubated with 5 mL of LB medium at 30°C, and 0.1 mM IPTG was added at 5 h of incubation. The strain was further cultivated for 20 h.
[b] *Ochrobactrum* sp. AIU 033 was incubated with 5 mL of 1,2-propanediol medium (pH 6.0) at 30°C for 2 days.
[c] Glycolic acid oxidase activity was assayed under standard assay conditions using crude enzyme solutions (5). The data are mean ± SD (n = 3).

The $K_m$ value for glycolic acid was 377 ± 59.2 mM and the $V_{max}$ value was 25.8 ± 3.37 nmol/min/mg protein, both of which are higher than those of native OcAOD: $K_m$ 167 mM and $V_{max}$ 11.3 nmol/min/mg protein (7).

**The thermal stability and pH stability of the recombinant enzyme** When the recombinant enzyme was incubated at 20°–60°C for 20 min at pH 6.0, more than 80% of the enzyme activity remained below 30°C and decreased along with the increase in the incubation temperature (Fig. 4A). In addition, 40% of the enzyme activity remained by incubation of the recombinant enzyme at 50°C, whereas native OcAOD was completely denatured at 50°C (7).

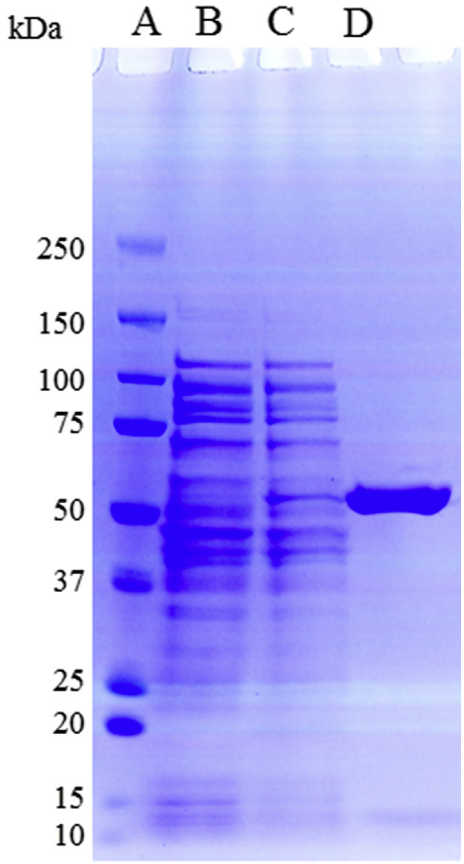


FIG. 3. SDS-PAGE of recombinant OcAOD. Lane A, standard proteins; lane B, cell-free extract from *E. coli* BL21(DE3); lane C, cell-free extract from recombinant *E. coli* BL21(DE3) harboring pTA-OcAOD; lane D, purified recombinant OcAOD.

**TABLE 2.** Substrate specificity of recombinant OcAOD.

| Compound | Relative activity (%) |
|---|---|
| Glycolic acid | 100 |
| Glyoxylic acid | 0 |
| Methanol | 0 |
| Ethanol | 16.4 ± 0.39 |
| 1-Propanol | 55.9 ± 0.31 |
| 1-Butanol | 253 ± 42.7 |
| 1-Pentanol | 314 ± 32.6 |
| 1-Hexanol | 197 ± 8.38 |
| 1-Octanol | 180 ± 6.44 |

Oxidase activity for the indicated compounds was assayed under standard assay conditions using 200 mM compounds except l-butanol (100 mM), 1-pentanol (100 mM), 1-hexanol (10 mM), 1-octanol (2 mM) (5). The enzyme exhibiting 2 munits/ml of activity for glycolic acid was used. The data are mean ± SD (n = 3).

We analyzed the pH stability by incubation at 25°C for 20 min in the pH range of 5.0–8.0. More than 80% of the enzyme activity remained at the pH range of 5.0–6.0, and 68% and 36% of the enzyme activity remained after incubation at pH 7.0 and 8.0, respectively (Fig. 4B). However, native OcAOD showed the highest stability at pH 6.0 (7).

Although some enzymatic properties of the recombinant enzyme differed from those of native OcAOD, the recombinant enzyme showed glycolic acid oxidase activity, a molecular weight, and substrate specificity that are similar to those of native OcAOD. We thus concluded that the ORF1 and ORF2 encode the precursor for the β-subunit of OcAOD (pro-AodB) and the α-subunit of OcAOD (AodA), respectively.

**Proteins homologous to sequences of pro-AodB and AodA** The deduced amino acid sequence of the pro-AodB gene (*aodB*), which is located upstream of the AodA gene (*aodA*), showed high similarity to the putative signal peptides for the Tat pathway from *Ochrobactrum* sp. EGD-AQ16 (accession no. WP_021587704.1) (183/184, 99% identity), *Mesorhizobium* sp. LNHC232B00 (accession no. WP_023764834.1) (147/182, 81% identity), and hypothetical proteins from *Ochrobactrum intermedium* (accession no. WP_006471203.1) (183/189, 97% identity) and *O. anthropi* ATCC 49188 (accession no. WP_001368621.1) (179/184, 97% identity) (16). The consensus sequence for the Tat pathway (SRRDILKR) (21) was identified in the N-terminal region of aa 17–24 of pro-AodB (Fig. S2A).

The deduced amino acid sequence of AodA showed high similarity to that of the putative GMC oxidoreductases from *Ochrobactrum* EGD-AQ16 (accession no. WP_006471204.1) (518/523, 99% identity) and *O. anthropi* ATCC 49188 (accession no. WP_001368620.1) (512/523, 98% identity) (16) and the putative 2-keto-gluconate dehydrogenases from *O. intermedium* (accession no. WP_006465776.1) (518/535, 97% identity) and *Mesorhizobium* sp. LNHC232B00 (accession no. WP_023764835.1) (433/523, 83% identity). In addition, the flavin-binding motif (GXGXXG) (22) was confirmed at the position of 17–22 aa from the N-terminus of AodA. The GMC oxidoreductase motifs were also found in the regions of 19–304 aa and 391–509 aa of AodA (Fig. S2B).

**The localization of recombinant OcAOD in *E.coli*** Since we identified the consensus sequence for the Tat pathway in the N-terminal region of pro-AodB, we analyzed the localization of recombinant OcAOD in *E. coli*. First, we prepared the spheroplast and periplasm fractions from recombinant *E. coli* harboring *aodB* and *aodA* (*E. coli*/pTA-OcAOD). The recombinant *E. coli* harboring only *aodA* [*E. coli*/pTA-OcAOD(Δ*aodB*)] was also used to investigate the effect of *aodB* on localization of OcAOD. The successful fractionations were confirmed by the measuring 1,2-propanediol oxidoreductase activity as a cytoplasmic enzyme (23) and the β-lactamase activity as a periplasmic enzyme (19), respectively. The 1,2-propandiol oxidation activities of the spheroplast fractions were 25.6 munits/mL (*E. coli*/pTA-OcAOD) and 20.9 munits/mL [*E. coli*/pTA-OcAOD(Δ*aodB*)], whereas the periplasm fractions showed no activity (*E. coli*/pTA-OcAOD) and 2.05 munits/mL [*E. coli*/pTA-OcAOD(Δ*aodB*)] (Table 3). In contrast, the β-lactamase activities of the spheroplast fractions were 0.11 units/mL (*E. coli*/pTA-OcAOD) and 0.16 units/mL [*E. coli*/pTA-

**TABLE 3.** Enzyme activities of spheroplast and periplasm fractions from recombinant *E. coli* BL21(DE3) harboring pTA-OcAOD or pTA-OcAOD(Δ*aodB*).

| Strain | Fraction | Activity | | |
|---|---|---|---|---|
| | | Glycolic acid oxidase (mU/mL) | 1,2-Propanediol dehydrogenase (mU/mL) | β-Lactamase (U/mL) |
| *E. coli* BL21(DE3)/pTA-OcAOD | Spheroplast | 0 | 25.6 ± 8.91 | 0.11 ± 0.04 |
| | Periplasm | 0.71 ± 0.13 | 0 | 1.38 ± 0.51 |
| *E. coli* BL21(DE3)/pTA-OcAOD (Δ*aodB*) | Spheroplast | 0 | 20.9 | 0.16 |
| | Periplasm | 0 | 2.05 | 2.49 |

The data are mean ± SD (n = 3). 1,2-Propanediol oxidoreductase and β-lactamase localized in spheroplast and periplasm, respectively (18,22).

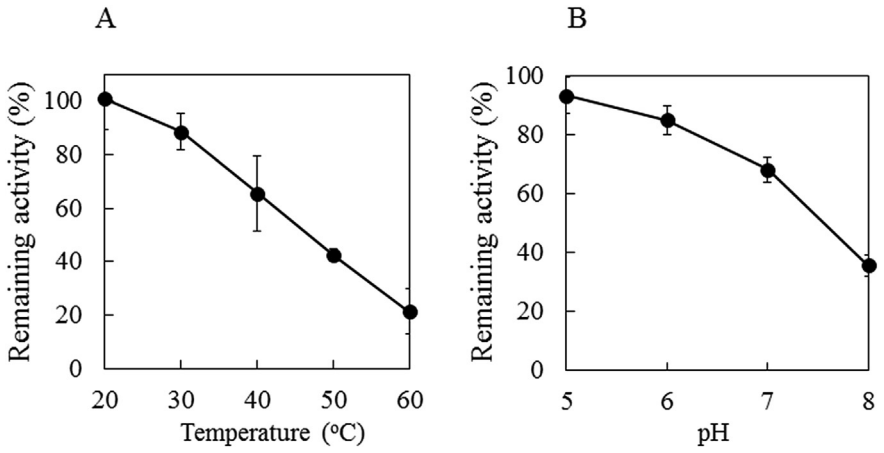


FIG. 4. The thermal stability and the pH stability of recombinant OcAOD. Experimental conditions are same as experiments of native OcAOD (7). (A) The thermal stability was assayed under standard assay conditions after the enzyme solution was incubated at pH 6.0 for 20 min at the indicated temperatures. The percentage of remaining activity was obtained by determining the ratio to activity without incubation. (B) The pH stability was assayed under standard conditions after incubation at 25°C for 20 min at the indicated pH. The percentage of remaining activity was obtained as a ratio to that without incubation. The data are mean ± SD (n = 3).

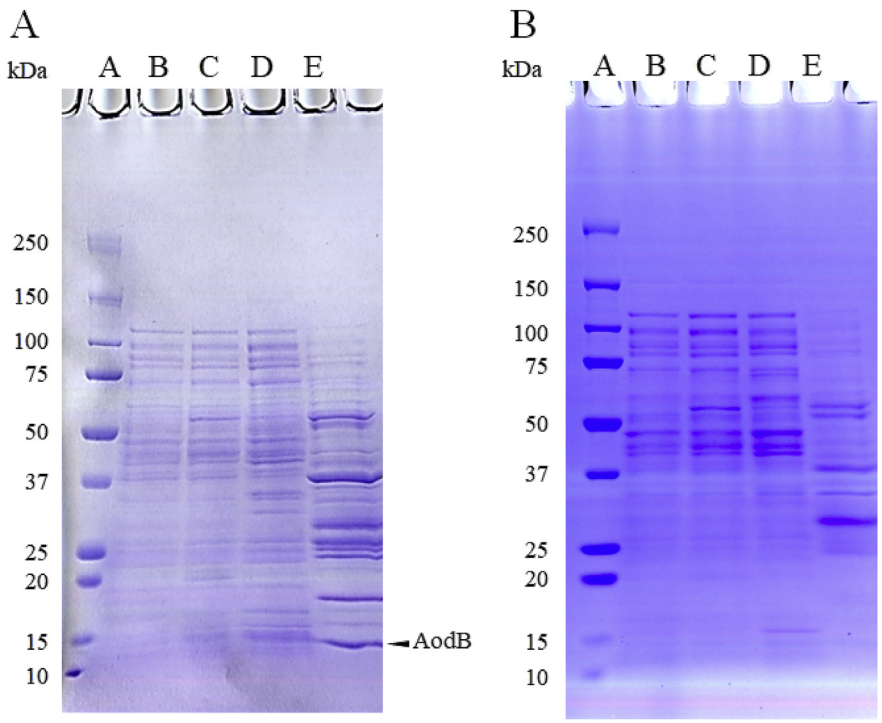


FIG. 5. SDS-PAGE using spheroplast and periplasm fractions of recombinant *E. coli* harboring pTA-OcAOD (A) and pTA-OcAOD(Δ*aodB*) (B). Lane A, standard proteins; lane B, cell-free extract from *E. coli* BL21(DE3); lane C, cell-free extract from recombinant *E. coli* BL21(DE3) harboring pTA-OcAOD or pTA-OcAOD(Δ*aodB*); lane D, spheroplast fraction from recombinant *E. coli* BL21(DE3) harboring pTA-OcAOD or pTA-OcAOD(Δ*aodB*); lane E, periplasm fraction from recombinant *E. coli* BL21(DE3) harboring pTA-OcAOD or pTA-OcAOD(Δ*aodB*).

OcAOD(Δ*aodB*)], and those of the periplasm fractions were 1.38 units/mL (*E. coli*/pTA-OcAOD) and 2.49 units/mL [*E. coli*/pTA-OcAOD(Δ*aodB*)]. Since we were able to confirm the successful fractionations, we used both the spheroplast and periplasm fractions to analyze the localization of AodA and AodB in *E. coli*.

According to comparisons of SDS-PAGE using the spheroplast and periplasm fractions between *E. coli*/pTA-OcAOD and *E. coli*/pTA-OcAOD(Δ*aodB*), remarkable protein band with the same molecular mass of AodA (52 kDa) was not found in spheroplast fractions(Fig. 5A,B, lane D), and endogenous proteins of 52 kDa were present in periplasm fractions as a remarkable protein band (Fig. 5A,B, lane E). Thus, localization of AodA was not decided in our experiment. However, protein band with the same molecular mass of AodB (14 kDa) were significantly recognized on SDS-PAGE in the only periplasm fraction of *E. coli*/pTA-OcAOD (Fig. 5A, lane E). In addition, the oxidase activity for glycolic acid was detected in the periplasm fraction (0.71 munits/mL) of *E. coli*/pTA-OcAOD, but not in the spheroplast fraction (Table 3). Based on these results, we concluded that the active form of OcAOD would be localized in the periplasm.

**Effects of the co-expression of *tatABC*, *aodB*, and *aodA* in *E. coli* on OcAOD productivity** Proteins containing the Tat signal are transported from the cytoplasm to the periplasm through TatABC protein (24). It was also reported that the overexpression of *tatABC* and *tatAC* improved the Tat-dependent protein secretion in *Corynebacterium glutamicum* (25) and *Streptomyces griseus* (26). To increase the productivity of the active form of OcAOD in recombinant *E. coli*, we co-expressed *aodB*, *aodA*, and *tatABC* by a single plasmid, pTA-OcAOD-TatABC, and we measured the OcAOD productivity. Recombinant *E. coli* BL21(DE3) harboring pTA-OcAOD-TatABC produced 265 munits of glycolic acid oxidase activity in the cells of 1 L of culture broth by IPTG induction (Table 1). The OcAOD productivity increased by 1.2-fold by the co-expression of *tatABC* compared to that of recombinant *E. coli* harboring only pTA-OcAOD.

## DISCUSSION

We cloned the set of genes encoding OcAOD, which catalyzes the oxidation of glycolic acid to glyoxylic acid. The set of genes for OcAOD contained two ORFs consisting of 555 bp (*aodB* encoding pro-AodB) and 1572 bp (*aodA* encoding AodA) segments beside each other (Fig. 2). There are no homologous enzymes, which have been experimentally characterized, of pro-AodB and AodA, suggesting that our research first characterized this type of AOD. The deduced amino acid sequence of AodA showed high similarity to those of putative GMC oxidoreductases and putative 2-keto-gluconate dehydrogenase, and it contained the GMC oxidoreductase motif and the flavin-binding motif (Fig. S2B). The recombinant OcAOD expressed in *E. coli* showed oxidase activity toward primary alcohol with C2–C8 (Table 2).

It is known that the AODs belonging to the GMC family show oxidase activity toward short- and medium-chain primary alcohols or allyl alcohols (27). OcAOD would therefore belong to the GMC oxidoreductase family, and AodA can be expected to play an important role in the enzyme activity.

Pro-AodB was revealed to possess the consensus sequence for the Tat pathway (SRRDILKR) at the position 17–24 of pro-AodB (Fig. 2 and S2A, gray box sequence inside the deduced amino acid sequence of pro-AodB). In addition, the N-terminal sequencing of the β-subunit of native OcAOD revealed that its N-terminus was located at the position 50–79 of pro-AodB (Fig. 2 and S2A, black box sequence inside the deduced amino acid sequence of pro-AodB). The estimated molecular mass of pro-AodB from aa 50–184 is also in agreement with that of the β-subunit of native OcAOD (14 kDa).

In light of these results, we speculated that the position aa 1–49 of pro-AodB (Figs. 2 and S2A, double underlining) is removed as a

signal peptide along with an export to the periplasm through the Tat pathway. This hypothesis was supported by the results of our enzyme activity measurement and SDS-PAGE of the spheroplast and periplasm fractions using recombinant *E. coli* that expressed the *aodB* and *aodA*: glycolic acid oxidase activity was observed in the periplasm fraction but not in the spheroplast fraction (Table 3), and the SDS-PAGE of the periplasm fraction showed the 14-kDa protein band derived from AodB (Fig. 5A).

Rodrigue et al. (28) demonstrated that the periplasmic nickel-containing hydrogenases (which are composed of a small subunit containing a Tat pathway signal sequence and a large subunit devoid of an export signal) naturally required a small subunit for membrane translocation in *E. coli*. This mechanism is referred to as the hitchhiker co-translocation mechanism, and there are a few enzymes of this type among the Tat-dependent enzymes. We predicted that the export of OcAOD to the periplasm takes place by the same mechanism. Furthermore, it was reported that the small subunit of the nickel-containing hydrogenases is required not only for membrane translocation but also for the acquisition of nickel (28). AodB of OcAOD would play the same role in acquisition of cofactor (flavin and/or ion).

The Tat pathway serves to actively translocate folded proteins across a membrane, whereas general secretion route, termed Sec-pathway, transports proteins in an unfolded manner. OcAOD contains flavin and ion atom as cofactors (7), and AodA has the flavin-binding motif. The membrane translocation mechanism by Tat pathway is necessary for that OcAOD can bind to cofactors, because flavin and ion atom mainly presents in cytoplasm.

The OcAOD productivity was increased by the heterologous expression of *aodB* and *aodA* in *E. coli*, and further increased by co-expression with *tatABC*, which is present in the inner membrane and performs key functions in protein translocation (24) (Table 1). These results indicated that the co-expression of *tatABC* in the inner membrane would assist the exporting of OcAOD into the periplasm. In fact, high yields of green fluorescent protein fused to a Tat-dependent enzyme, trimethylamine *N*-oxide reductase (TorA), from *E. coli* as confirmed by the overexpression of *tatABC* in the recombinant *E. coli* (29,30). In other microorganisms, it was reported that the overexpression of *tatABC* enhanced the secretion of pro-protein glutaminase from *Chryseobacterium proteolyticum* and pro-transglutaminase from *Streptomyces mobaraensis*, which are fused with the Tat signal of TorA in *C. glutamicum* (25). Overexpression of *tatAC* also enhanced endogenous hydrolases in *S. griseus* (26). In our experiments, most of the recombinant OcAOD was exported to periplasm in *E. coli* harboring pTA-OcAOD. Thus, it would be expected that co-expression with *tatABC* is more effective in increasing the enzyme productivity when the expression level of OcAOD is enhanced in the cytoplasm of *E. coli*.

With respect to the enzymatic properties of the recombinant OcAOD, the enzyme showed oxidase activity for glycolic acid but not for glyoxylic acid (Table 2), indicating that the recombinant OcAOD is as useful for glyoxylic acid production as native OcAOD. Although the substrate specificity of the recombinant OcAOD was similar to that of native OcAOD, our results also demonstrated differences in enzymatic properties between the recombinant and native OcAOD. These differences in enzymatic properties would be due to differences of expression conditions in the host microorganism. One possibility is that difference in cofactor contents (flavin and iron) of recombinant OcAOD was caused in *E. coli*. The higher $K_m$ and $V_{max}$ values of the recombinant OcAOD would be advantageous for a more rapid conversion of glycolic acid into glyoxylic acid under the reaction conditions with a high concentration of glycolic acid. If an inhibition of enzyme reaction was caused by high concentration of glycolic acid, OcAOD with high $K_m$ value would avoid the substrate inhibition. The pH stability and thermal stability of the recombinant OcAOD also differed from those of native OcAOD. Notably, the recombinant OcAOD showed higher thermal stability than native OcAOD. Since high thermal stability is advantageous for long−term reactions, the recombinant OcAOD would be effective from the perspective of applications to glyoxylic acid production.

In conclusion, we constructed a heterologous expression system of OcAOD in *E. coli*, and our experimental findings indicated the localization of the active form of recombinant OcAOD. These results and those of our amino acid sequencing analysis of each subunit of OcAOD provide the predicted function of the β-subunit in the hitchhiker co-translocation mechanism of OcAOD through the Tat pathway. Our results also demonstrated that (i) the OcAOD productivity of recombinant *E. coli* BL21(DE3) harboring pTA-OcAOD-TatABC was approximately 30-fold higher than that of *Ochrobactrum* sp. AIU 033, and (ii) the recombinant OcAOD has preferable properties for the enzymatic synthesis of glyoxylic acid from glycolic acid. These results will contribute to future studies aimed at improving enzyme productivity.

Supplementary data to this article can be found online at https://doi.org/10.1016/j.jbiosc.2018.12.012.

## ACKNOWLEDGMENTS

This work was supported by a JSPS KAKENHI Grant-in-Aid for Young Scientists (B) no. JP 25820395, a Grant-in-Aid for Scientific Research (C) no. JP 18K11704 (to M. Yamada), a Grant-in-Aid for Scientific Research (B) no. JP 15KT0073, a Grant-in-Aid for Scientific Research (B) no. JP 17H02209 (to K. Nishiyama), and the Foundation for Japanese Chemical Research (to M. Yamada).

## References

1. **O'Neil, M. J., Heckelman, P. E., Koch, C. B., and Roman, K.:** The Merck index: an encyclopedia of chemicals, drugs, and biologicals, 14th ed. Merck Research Laboratories, Division of Merck & Co., Whitehouse Station, NJ (2006).
2. **Seip, J. E., Fager, S. K., Gavagan, J. E., Gosser, L. W., Anton, D. L., and Di Cosimo, R.:** Biocatalytic production of glyoxylic acid, J. Org. Chem., **58**, 2253−2259 (1993).
3. **Seip, J. E., Fager, S. K., Gavagan, J. E., Anton, D. L., and Di Cosimo, R.:** Glyoxylic acid production using immobilized glycolate oxidase and catalase, Bioorg. Med. Chem., **2**, 371−378 (1994).
4. **Gavagan, J. E., Fager, S. K., Seip, J. E., Payne, M. S., Anton, D. L., and Di Cosimo, R.:** Glyoxylic acid production using microbial transformant catalysts, J. Org. Chem., **60**, 3957−3963 (1995).
5. **Isobe, K.:** Oxidation of ethylene glycol and glycolic acid by glycerol oxidase, Biosci. Biotechnol. Biochem., **59**, 576−581 (1995).
6. **Yamada, M. and Isobe, K.:** A novel microbial aldehyde oxidase applicable to production of useful raw materials, glycolic acid and glyoxylic acid, from ethylene glycol, OMICS Int. Ferment. Technol., **4**, 116 (2015).
7. **Yamada, M., Higashiyama, T., Kishino, S., Kataoka, M., Ogawa, J., Shimizu, S., and Isobe, K.:** Novel alcohol oxidase with glycolate oxidase activity from *Ochrobactrum* sp. AIU 033, J. Mol. Catal. B Enzym., **105**, 41−48 (2014).
8. **Isobe, K. and Nishise, H.:** Enzymatic production of glyoxal from ethylene glycol using alcohol oxidase from methanol yeast, Biosci. Biotechnol. Biochem., **58**, 170−173 (1994).
9. **Isobe, K., Kato, A., Ogawa, J., Kataoka, M., Iwasaki, A., Hasegawa, J., and Shimizu, S.:** Characterization of alcohol oxidase from *Aspergillus ochraceus* AIU 031, J. Gen. Appl. Microbiol., **53**, 177−183 (2007).
10. **Isobe, K., Takahashi, T., Ogawa, J., Kataoka, M., and Shimizu, S.:** Production and characterization of alcohol oxidase from *Penicillium purpurescens* AIU 063, J. Biosci. Bioeng., **107**, 108−112 (2009).
11. **Isobe, K., Kato, A., Sasaki, Y., Suzuki, S., Kataoka, M., Ogawa, J., Iwasaki, A., Hasegawa, J., and Shimizu, S.:** Purification and characterization of a novel alcohol oxidase from *Paenibacillus* sp. AIU 311, J. Biosci. Bioeng., **104**, 124−128 (2007).
12. **Sasaki, Y., Isobe, K., Kataoka, M., Ogawa, J., Iwasaki, A., Hasegawa, J., and Shimizu, S.:** Purification and characterization of a new aldehyde oxidase from *Pseudomonas* sp. AIU 362, J. Biosci. Bioeng., **106**, 297−302 (2008).
13. **Yamada, M., Adachi, K., Ogawa, N., Kishino, S., Ogawa, J., Kataoka, M., Shimizu, S., and Isobe, K.:** A new aldehyde oxidase catalyzing the conversion of glycolaldehyde to glycolate from *Burkholderia* sp. AIU 129, J. Biosci. Bioeng., **119**, 410−415 (2015).

14. **Isobe, K., Watabe, S., and Yamada, M.:** Characterization and application of a glycolate dehydrogenase from *Trichoderma harzianum* AIU 353, J. Mol. Catal. B Enzym., **83**, 94–99 (2012).
15. **Sambrook, J., Fritsch, E. F., and Maniatis, T.:** Molecular cloning: a laboratory manual, 2nd ed. Cold Spring Harbor Laboratory Press, Cold Spring Harbor, NY (1989).
16. **Chain, P. S., Lang, D. M., Comerci, D. J., Malfatti, S. A., Vergez, L. M., Shin, M., Ugalde, R. A., Garcia, E., and Tolmasky, M. E.:** Genome of *Ochrobactrum anthropi* ATCC 49188 T, a versatile opportunistic pathogen and symbiont of several eukaryotic hosts, J. Bacteriol., **193**, 4274–4275 (2011).
17. **Osborn, M. J., Gander, J. E., Parisi, E., and Carson, J.:** Mechanism of assembly of the outer membrane of *Salmonella typhimurium*. Isolation and characterization of cytoplasmic and outer membrane, J. Biol. Chem., **247**, 3962–3972 (1972).
18. **Boronat, A. and Aguilar, J.:** Rhamnose-induced propanediol oxidoreductase in *Escherichia coli*: purification, properties, and comparison with the fucose-induced enzyme, J. Bacteriol., **140**, 320–326 (1979).
19. **Minsky, A., Summers, R. G., and Knowles, J. R.:** Secretion of beta-lactamase into the periplasm of *Escherichia coli*: evidence for a distinct release step associated with a conformational change, Proc. Natl. Acad. Sci. USA, **83**, 4180–4184 (1986).
20. **Laemmli, U. K.:** Cleavage of structure proteins during the assembly of the head of bacteriophage T4, Nature, **227**, 680–685 (1970).
21. **Berks, B. C.:** A common export pathway for proteins binding complex redox cofactors? Mol. Microbiol., **22**, 393–404 (1996).
22. **Dym, O. and Eisenberg, D.:** Sequence-structure analysis of FAD-containing proteins, Protein Sci., **10**, 1712–1728 (2001).
23. **Chen, Y. M. and Lin, E. C.:** Post-transcriptional control of L-1,2-propanediol oxidoreductase in the L-fucose pathway of *Escherichia coli* K-12, J. Bacteriol., **157**, 341–344 (1984).
24. **Sargent, F., Berks, B. C., and Palmer, T.:** Pathfinders and trailblazers: a prokaryotic targeting system for transport of folded proteins, FEMS Microbiol. Lett., **254**, 198–207 (2006).
25. **Kikuchi, Y., Itaya, H., Date, M., Matsui, K., and Wu, L. F.:** TatABC overexpression improves *Corynebacterium glutamicum* Tat-dependent protein secretion, Appl. Environ. Microbiol., **75**, 603–607 (2009).
26. **Chi, W. J., Oh, E. A., Kim, J. H., and Hong, S. K.:** Enhancement of protein secretion by TatAC overexpression in *Streptomyces griseus* Biotechnol, Bioprocess Eng., **16**, 59–71 (2011).
27. **Goswami, P., Chinnadayyala, S. S., Chakraborty, M., Kumar, A. K., and Kakoti, A.:** An overview on alcohol oxidases and their potential applications, Appl. Microbiol. Biotechnol., **97**, 4259–4275 (2013).
28. **Rodrigue, A., Chanal, A., Beck, K., Muller, M., and Wu, L. F.:** Co-translocation of a periplasmic enzyme complex by a hitchhiker mechanism through the bacterial tat pathway, J. Biol. Chem., **274**, 13223–13228 (1999).
29. **Matos, C. F., Branston, S. D., Albiniak, A., Dhanoya, A., Freedman, R. B., Keshavarz-Moore, E., and Robinson, C.:** High-yield export of a native heterologous protein to the periplasm by the tat translocation pathway in *Escherichia coli*, Biotechnol. Bioeng., **109**, 2533–2542 (2012).
30. **Thomas, J. D., Daniel, R. A., Errington, J., and Robinson, C.:** Export of active green fluorescent protein to the periplasm by the twin-arginine translocase (Tat) pathway in *Escherichia coli*, Mol. Microbiol., **39**, 47–53 (2001).